6TH INTERNATIONAL CONFERENCE ON FLOOD MANAGEMENT
September 2014 - São Paulo - Brazil
ICFM6

NONSTATIONARITY OF FLOODS IN THE ITAJAÍ-AÇU RIVER, IN BRAZIL

A.T. Silva[1], M.M. Portela[1] and M. Naghettini[2]
1. *CEHIDRO, Instituto Superior Técnico, Portugal*
2. *Federal University of Minas Gerais, Brazil*

ABSTRACT: Nowadays there seems to be a consensus among the scientific community that, due to climate change, there is an intensification of the hydrological cycle, which, coupled with evidence of the impact of persistent modes of regional climate variability, have led hydrologists to study hydrological extremes under nonstationarity. In this paper, the peaks-over-threshold (POT) model with Poisson arrivals and generalized Pareto (GP) distributed exceedances is used to assess the influence of El-Niño Southern Oscillation (ENSO) in the flood regime of the Itajaí-Açu river, in Southern Brazil. The application of the POT approach has the advantage of being able to detect and model the influence of climate on the occurrence rate of floods and their peak magnitudes separately.

Key Words: Flood frequency analysis, peaks-over-threshold, nonstationarity, ENSO

1. INTRODUCTION

Historically, flood frequency analysis has been applied under the assumption of stationarity. Recently, however, there is an increasing scientific consensus on climate change and the intensification of the hydrological cycle, assumably leading to changes in flood regimes. Milly et al. (2008) argue that such changes undermine stationarity in water resources engineering. Clarke (2007) questions the widespread assumption of stationarity in hydrological practice and contends that the next few decades should see an increase in the understanding in the drivers of change in flood regimes, not only for forecasting their development, but also for predicting the frequency of occurrence of extremes.

There is a number of recent studies that link changes in the regime of hydrological extremes to changes in teleconnection climate indices such as the North Atlantic Oscillation (NAO) and the El Niño – Southern Oscillation (ENSO) (Silva et al., 2012, 2013; Grimm and Tedeschi, 2009). Such signs of changes prompted the development of advances in the statistical methods applied to frequency analysis of extremes in order to account for the dynamic behavior of the data. Recently, nonstationary modeling of hydrological extremes, such as floods, has become an emerging topic of high scientific interest (Katz, 2010, 2013; Salas and Obeysekera, 2013, Silva et al., 2012, 2013).

In flood frequency analysis, the peaks-over-threshold (POT) framework is an alternative to the more popular annual maximum series approach in that it consists of sampling all the independent peak values above a given threshold and their annual arrival counts. A POT model enables the joint characterization of both the over-threshold peaks and their occurrence rate, thus resulting in a single distribution of annual maximum floods (Silva et al., 2013).

The generalized Pareto (GP) distribution is commonly adopted to model the exceedance magnitudes. Justification for its use arises from extreme value theory (Coles, 2001). Shane and Lynn (1964) proposed that the arrivals of over-threshold peaks conform to a Poisson process, hence they propose the Poisson distribution to model the annual number of peaks.

The combination of the Poisson and GP distributions in a POT framework results in a generalized extreme value (GEV) distribution for annual maxima (Davison and Smith, 1990).

Coles (2001) popularized parametric nonstationary GEV and GP models which allow the estimation of parameters as linear functions of covariates, through link functions.

This paper presents a study on the nonstationarity of floods in the Itajaí-açu river in Southern Brazil using a POT framework. The Poisson-GP model is used and nonstationarity is introduced separately in the Poisson and GP parameters, in order to model climate-flood links.

2. STUDY REGION AND DATA

The Itajaí river basin is located in the Santa Catarina State, in the South of Brazil and drains into the Atlantic Ocean. The total catchment area of the basin is approximately 15000 km^2. As shown in Fig. 1, there are two main tributaries that merge just 7 km from the ocean: the Itajaí-açu and the Itajaí-mirim rivers. According to Nery et al. (2000), rainfall in the Itajaí basin has a seasonal behavior comprehending two seasons: a wet season (October to March) and a relatively drier season (April – September).

The lower reaches of the Itajaí-açu river are prone to severe flooding (Martins and Clarke, 1993). In July 1983, an extreme flood caused extensive damage (US$1.1 bn) to the city of Blumenau and several fatalities (Tachini, 2010). The history of devastating floods in the Itajaí river basin motivated the construction of contention dams on the higher reaches of the river during the 1970s-90s (Abers, 2007). The first dam, identified in Fig. 1 as R1, in the Itajaí do Oeste tributary, was completed in 1973; the second, R2, in the Itajaí do Sul, was completed in 1975; the third, R3, in the Itajaí do Norte, was completed in 1992.

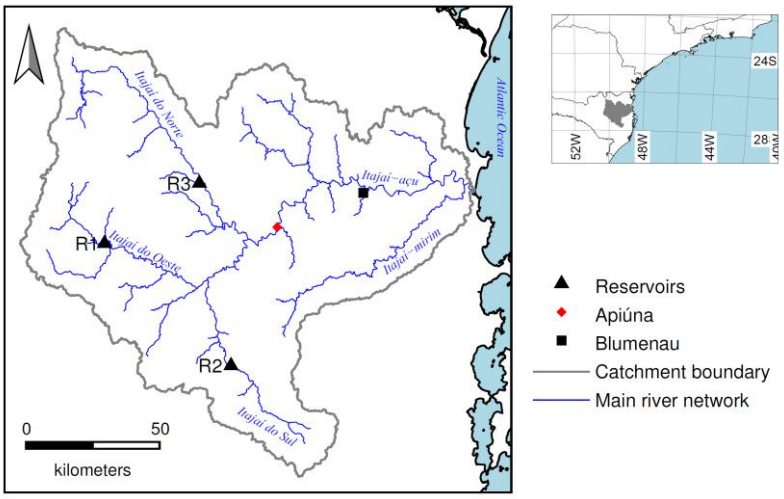

Figure 1: Itajaí river basin. Location of the utilized gauging station and existing flood control reservoirs.

The Itajaí basin is located within the Southeastern South America (SESA) region, where the influence of ENSO in climate variability has been reported (Grimm and Tedeschi, 2009). Grimm (2011) detected the influence of ENSO on the frequency and magnitude of heavy rainfall events in SESA. The 1983 historic flood in Blumenau is associated with an El Niño occurrence (Martins and Clarke, 1993).

The research carried out in this paper consists of an analysis on the influence of ENSO on the flood regime in the Itajaí-açu river. For that purpose, mean daily flow data from 1934/35 to 1990/91 at Apiúna (Fig. 1) were utilized. The catchment area at Apiúna is approximately 9242 km^2. The hydrologic year

beginning on October 1st was adopted so as to coincide with the beginning of the wet season. The data were collected by the Brazilian National Water Agency, ANA, and made available via the HIDROWEB database (http://hidroweb.ana.gov.br/).

The utilized ENSO data consists of the monthly Niño3.4 climate index calculated from the HadISST1 dataset by Rayner et al. (2003), which refers to the sea surface temperature (SST) from 5S-5N and 170-120W, from 1870 on. The data were centered by subtracting the mean of the respective months. The annual ENSO index used in the analysis was defined as the December-to-February mean value (DJF) of the centered Niño3.4 SST.

A preliminary analysis was made on the potential influence the three reservoirs of the Itajaí-açu tributaries may have on the flood regime of Apiúna, in which a representative flood volume is compared to the capacity of the flood control reservoirs. Table 1 shows the capacities and catchment areas of the 3 reservoirs shown in Fig. 1 (Tachini, 2010). The representative flood volume was obtained by averaging the dimensionless hydrographs of 184 independent floods and multiplying the resulting mean dimensionless hydrograph by the mean of the annual maximum series. The volume of the hypothetical flood was determined at 881.4×10^6 m^3. Upon comparing this value with the reservoir capacities on Table 1, it seems that reservoirs R1 and R2 do not significantly alter the flood regime at Apiúna. Reservoir R3 is, by far, the largest of the three, hence we admit that the combined effect of all three reservoirs on the flood regime at Apiúna (60% of the mean flood volume; 50% of the catchment area) may be significant. For that reason, only the data prior to the beginning of operation of R3 were utilized.

Table 1: Main characteristics of flood control reservoirs in the Itajaí-açu basin.

Reservoir	River	Operation started	Capacity (m^3)	Catchment area (km^2)
R1	Itajaí do Oeste	1973	83.0×10^6	1042
R2	Itajaí do Sul	1976	97.5×10^6	1273
R3	Itajaí do Norte	1992	357.0×10^6	2318

3. METHODS

3.1 Nonstationary Poisson-GP model

The Poisson-GP model is a common setup for flood frequency analysis under a POT approach. That model consists of a combined use of the Poisson distribution for modeling the annual number of flood occurrences, Y, and of the GP distribution for modeling the threshold exceedance magnitudes, X_{OT}. The probability mass function (PMF) of the Poisson distribution is given by

$$P(Y = y) = \exp(-y)\,\frac{\lambda^{y}}{y!}, \quad y = 0, 1, 2, \ldots \qquad [1]$$

where the Poisson parameter, λ, is estimated by the sample mean.

Cunnane (1979) and NERC (1975, pp. 197-198) propose a test for the verification of the Poisson assumption for Y, based on the dispersion index (ratio between sample variance and mean). If the data adjusts to the Poisson distribution, the dispersion index should take values close to 1.

The GP has the cumulative distribution function (CDF)

$$G(x) = 1 - \left[1 - \kappa\left(\frac{x-\mu}{\sigma}\right)\right]^{\frac{1}{\kappa}} \quad , \kappa \neq 0, x \geq \mu \qquad [2]$$

where κ, σ and μ are, respectively, the shape, scale and location parameters, being that the latter is fixed and equal to the selected threshold.

The selection of the threshold remains the most subjective aspect of POT modeling and there is no universally accepted rule for it. In this paper, the threshold is selected using the mean residual life (MRL) plot technique, described by Davison and Smith (1990) and Coles (2001). In order to ensure the independence of the POT data, it was imposed that the selected peaks must be separated in time by a minimum of 10 days, and that the streamflow between two peaks should decrease below as much as two thirds of the first one, after a suggestion by NERC (1975) and Cunnane (1979).

Under the Poisson assumption, the CDF of annual maximum floods, $F(x)$, is given by

$$F(x) = \exp\left\{-\lambda\left[1-G(x)\right]\right\} \qquad [3]$$

By combining [1] and [2], one obtains the CDF of the GEV model for annual maxima with a Poisson-GP parameterization

$$F(x) = \exp\left\{-\lambda\left[1-\kappa\left(\frac{x-\mu}{\sigma}\right)\right]^{\frac{1}{\kappa}}\right\} \quad ,\kappa \neq 0, x \geq \mu \qquad [4]$$

A pragmatic approach for POT modeling under nonstationarity is to allow the parameters of [4] to change over time as a function of a covariate, following that at any given point in time the annual maxima are described by an extreme value distribution, even if such distribution changes over time.

A varying Poisson parameter, λ, can be estimated parametrically using a generalized linear model (GLM, Davison, 2003) where the response variate, y, has a Poisson mass and the mean of y is related to one or more linear predictors through link functions.

Davison and Smith (1990) and Coles (2001) propose an approach for covariate modeling of the GP parameters in a POT context using regression. Similar to the GLM, the nonstationary GP model uses link functions of a covariate as linear predictors of the response, x. Usually, nonstationarity is only applied to the scale parameter of the GP, σ, and the shape parameter κ is assumed stationary, since the estimation of κ is difficult even under stationarity since data in the upper tail is very scarce.

Model selection under nonstationarity is an important issue. The basic aim here is to obtain a parsimonious model with the capacity of explaining much of the data variation. In this paper, the relative performances of candidate models, both stationary and nonstationary, were evaluated using: (i) asymptotic likelihood ratio tests (LRT, Coles, 2001), whenever possible; and (ii) the Akaike (1974) information criterion, AIC.

3.2 Uncertainty estimation

The methods described in 3.1 are subject to statistical uncertainty due to finite data samples of hydrologic random variables. In this paper, the delta method (Davison, 2003) was applied to estimate the uncertainty of estimated parameters and functions of those parameters, such as flood quantiles. According to the delta method, if $\hat{\boldsymbol{\theta}}$ is a k-parameter vector estimate of $\boldsymbol{\theta} = (\theta_1,\ldots,\theta_k)$, and $\boldsymbol{\Sigma}$ is the limiting variance-covariance matrix of the parameter estimators $\hat{\boldsymbol{\theta}}$, the asymptotic variance, V_g, of a scalar function $g(\boldsymbol{\theta})$ can be approximated by

$$V_g = \mathbf{h}^T \boldsymbol{\Sigma} \mathbf{h} \qquad [5]$$

where $\mathbf{h}$ is the gradient of $g(\hat{\boldsymbol{\theta}})$ and can be obtained either by algebraic or numerical differentiation.

An estimate of $\boldsymbol{\Sigma}$ can be obtained numerically by inverting the Hessian of the respective log-likelihood function at the point of maximum likelihood.

When dealing with the Poisson-GP model, it is convenient to separate the parameters of the Poisson from the parameters of the GP and assume that the sample properties of the flood peak magnitudes are independent of the flood occurrence process. Under the former assumption, we have $\boldsymbol{\theta} = (\boldsymbol{\theta}_{\mathbf{Poi}}, \boldsymbol{\theta}_{\mathbf{GP}})$, with $\mathrm{Cov}(\theta_{Poi\ i}, \theta_{GP\ j}) = 0$ and $\boldsymbol{\Sigma}$ becomes

$$\boldsymbol{\Sigma} = \begin{pmatrix} \boldsymbol{\Sigma}_{\mathbf{Poi}} & \mathbf{0}_{m,n} \\ \mathbf{0}_{n,m} & \boldsymbol{\Sigma}_{\mathbf{GP}} \end{pmatrix} \qquad [6]$$

where m and n are, respectively, the number of parameters of the Poisson and GP models, $\mathbf{0}_{m,n}$ is an m-by-n null matrix, and $\boldsymbol{\Sigma}_{\mathbf{Poi}}$ and $\boldsymbol{\Sigma}_{\mathbf{GP}}$ are the asymptotic variance-covariance matrices of the parameter estimators of the Poisson and GP, respectively.

4. RESULTS

4.1 Threshold selection

The threshold selected using the MRL plot technique, mentioned in 3.1, was $u_0 = 650\,m^3/s$. Fig. 2a shows the MRL plot, complemented with 95% confidence bands and theoretical GP MRL functions obtained using the methods described in Silva et al. (2013).

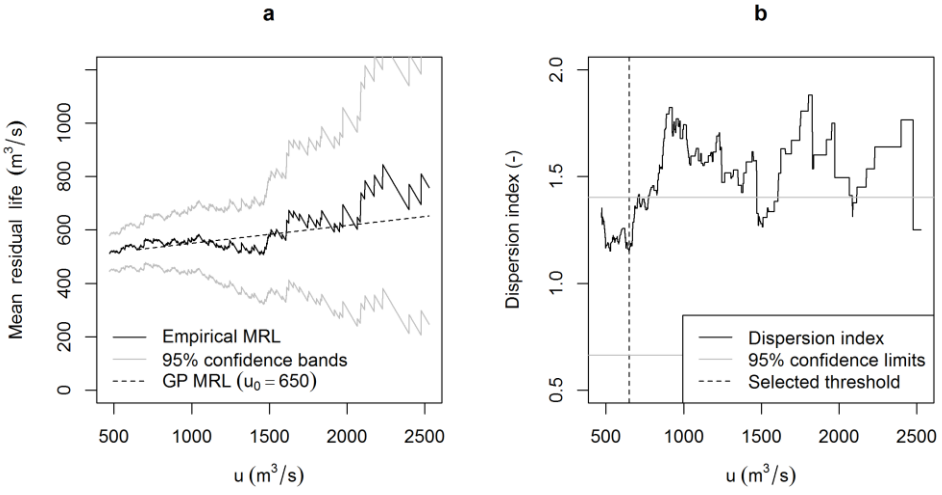

Figure 2: **a** Empirical MRL plot with 95% confidence band and theoretical GP MRL; **b** dispersion index plot.

Fig. 2b shows the dispersion index plot, obtained by computing the dispersion index for increasing values of the threshold, u. The plot was complemented with the confidence limits obtained using the methods

described in Silva et. al. (2013). That figure shows that the Poisson assumption should not be rejected for the selected threshold.

4.2 Over-threshold occurrence counts models

The (non)stationarity of the annual over-threshold occurrence counts, Y, were analyzed using the Niño3.4 (DJF) index as a potential covariate, z. Fig. 3a shows the observed values of Y plotted against the corresponding value of the covariate.

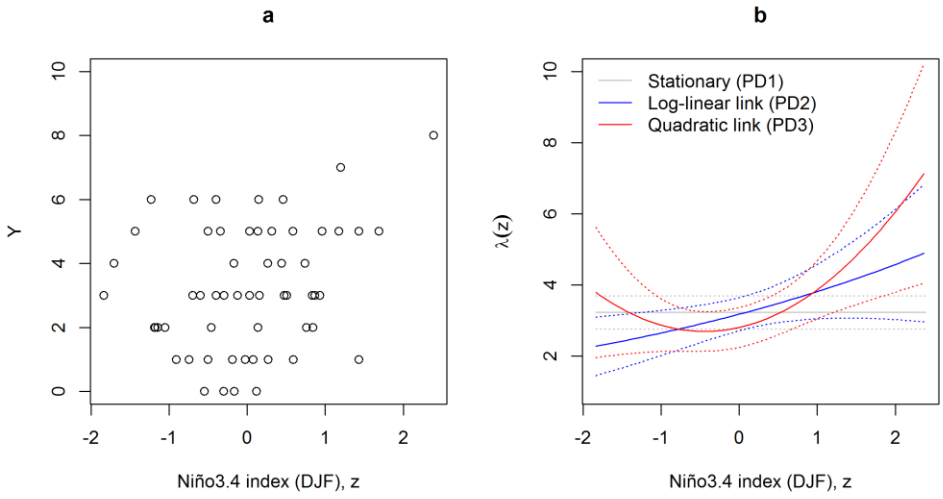

Fig. 3: **a** Annual number of over-threshold peak occurrences, Y, plotted against the Niño3.4 (DJF) index of the corresponding year. **b** Parametric GLM estimates of $\lambda(z)$ and 95% confidence envelopes (*dotted curves*).

The stationary Poisson model, PD1, was used as a baseline model. Based on a visual analysis of Fig 3a, two parametric GLM models with Poisson mass were postulated for describing the variation of the Poisson parameter as a function of the covariate, $\lambda(z)$: PD2 with a log-linear link, which is the canonical link function for a Poisson GLM, $\log\lambda(z) = \lambda_0 + \lambda_1 z$, and PD3 with the quadratic polynomial link $\lambda(z) = \lambda_0 + \lambda_1 z + \lambda_2 z^2$.

The parameter estimated and respective standard errors of the fitted models are presented in Table 2. Since PD1 is nested in both PD2 and PD3, we can apply an asymptotic LRT where PD1 in the null model to test whether or not the stationary model Pd1 should be rejected in favor of either of the nonstationary models PD2 or PD3. Table 2 shows the maximized log-likelihoods and p-values of the LRTs, as well as the AIC scores for each model. The p-values suggest that the stationary model PD1 should be rejected in favor of either PD2 or PD3 at the 5% significance level. The relative performance of models PD2 and PD3 cannot be evaluated through an LRT, however, according to AIC, PD3 provides the best fit for the data.

Fig. 3b shows the estimates of $\lambda(z)$ for the fitted models as well as their respective 95% confidence bands, which were constructed using the delta method.

Table 2: Parameter estimates and standard (st.) errors for the models fitted to the sample of annual number of over-threshold occurrences, Y, for $u_0 = 650\,m^3/s$; maximized log-likelihood and p-value for the LRT comparing a model (alternate) with the PD1 (null); AIC.

Model	Parameter estimate (st. error)	Max. log-likelihood	p-value	AIC
PD1 (Stationary λ)				
λ	3.2280 (0.2380)	-117.79		237.58
PD2 (log-linear $\lambda(z)$)				
λ_0	1.1556 (0.0749)	-115.50	0.03	235.00
λ_1	0.1824 (0.0849)			
PD3 (quadratic polynomial $\lambda(z)$)				
λ_0	2.8023 (0.2854)	-113.28	0.01	232.55
λ_1	0.4974 (0.3018)			
λ_2	0.5635 (0.2703)			

4.3 Over-threshold peak magnitudes models

In this section the relationship between the over-threshold peak magnitudes, X_{OT}, and the Niño3.4 covariate, z, is analyzed. This analysis focused on the scale parameter of the GP, σ, being that the shape parameter, κ, was considered a constant throughout the analyses. Fig. 4a shows the X_{OT} sample plotted against the covariate z. A visual analysis of that figure suggests that the relationship between X_{OT} and z is a complex one since it does not seem that the sampled flood peaks' statistical characteristics exhibit any monotonically increasing or decreasing behavior with regards to the covariate.

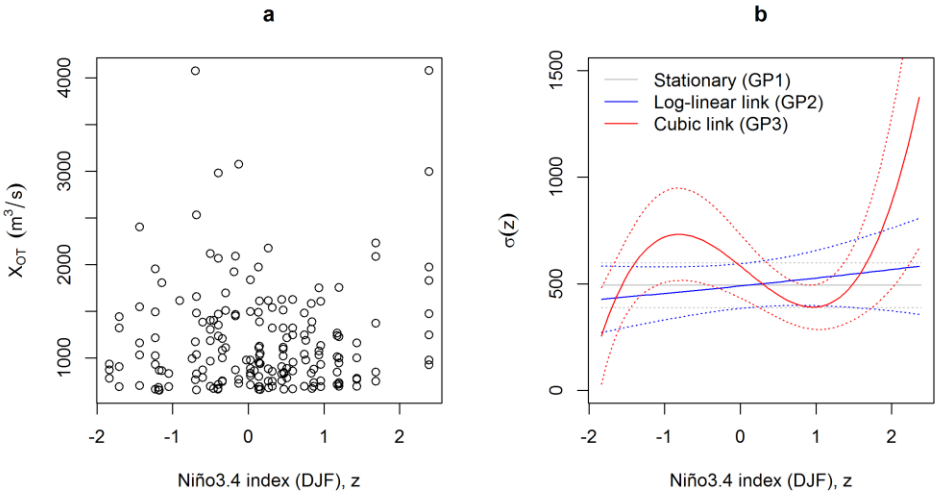

Figure 4: **a** Over-threshold peak magnitudes plotted against the Niño3.4 (DJF) index of the corresponding hydrological year. **b** Parametric GP estimates of $\sigma(z)$ and 95% confidence envelopes (*dotted curves*).

A stationary model, GP1 was considered as a baseline model. Based on a visual analysis of Fig. 4a, two parametric nonstationary GP models were postulated for describing $\sigma(z)$: GP2 with a log-linear link, $\log\sigma(z) = \sigma_0 + \sigma_1 z$, and GP3 with a cubic polynomial link, $\sigma(z) = \sigma_0 + \sigma_1 z + \sigma_2 z^2 + \sigma_3 z^3$.

Table 3 presents the parameter estimates and respective standard errors of the GP models. Since GP1 is nested in both GP2 and GP3, asymptotic LRTs were applied where GP1 is the null model. The results of Table 3 suggest: (i) the stationary model GP1 should not be rejected in favor of the nonstationary GP2 at the 5% significance level; (ii) GP1 should be rejected in favor of GP3 at 1% and 5% significance levels; (iii) according to the AIC, GP3 provides the best fit for the data.

Table 3: Parameter estimates and standard (st.) errors for the distributions fitted to the peak magnitudes above the threshold $u_0 = 650\,m^3/s$; maximized log-likelihood and p-value for the LRT comparing a model (alternate) with the GP1 (null); AIC.

Model	Parameter estimate (st. error)	Max. log-likelihood	p-value	AIC
GP1 (Stationary GP)				
$\mu = u_0$		-1337.2		2676.3
σ	493.7516 (53.3881)			
κ	-0.0627 (0.0792)			
GP2 (log-linear $\sigma(z)$)				
$\mu = u_0$		-1336.3	0.33	2678.6
σ_0	6.1943 (0.1092)			
σ_1	0.0732 (0.0750)			
κ	-0.0567 (0.0796)			
GP3 (cubic polynomial $\sigma(z)$)				
$\mu = u_0$		-1327.9	$< 10^{-3}$	2665.8
σ_0	583.4352 (76.1296)			
σ_1	-287.1907 (91.0245)			
σ_2	-27.8595 (35.2899)			
σ_3	123.0112 (36.1158)			
κ	0.0996 (0.0766)			

Fig. 4b shows the different estimates of $\sigma(z)$ as well as their respective 95% confidence envelopes, which were obtained using the delta method.

4.4 Annual maxima models

In this section, 2 models for annual maxima were considered, based on eqn. [3]: (i) a stationary model, AM1, obtained by combining the stationary Poisson and GP models, PD1 and GP1; (ii) a nonstationary model, AM2, obtained by combining the nonstationary Poisson and GP models, PD3 and GP3. Excluding the threshold, which is fixed in either case, models AM1 and AM2 have 3 and 8 parameters, respectively.

In Fig. 5a the AM1 model is compared against the observed AMS sample, which was plotted according to the Gringorten (1963) plotting position. Fig. 5b shows the observed annual maximum floods and flood quantiles with a non-exceedance probability, F, of 0.75 and 0.99, as a function of the Niño3.4 (DJF) index, z. Fig. 5b effectively illustrates the complex dependence structure between the probability of non-exceedance of annual maximum floods as a function of the utilized climate covariate, comprising a

quadratic relationship in $\lambda(z)$ and a cubic relationship in $\sigma(z)$. In Fig. 5a,b, the 5 largest observed annual maxima are dated and marked as filled circles.

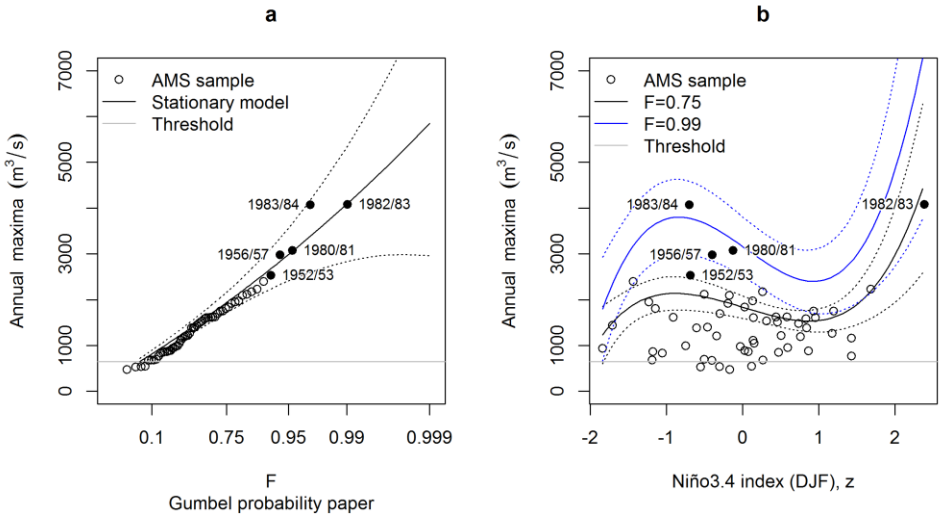

Figure 5: **a** AMS sample, AM1 model and 95% confidence envelopes (dotted curves). **b** AMS sample plotted against the corresponding Niño3.4 index; estimated quantiles for 2 non-exceedance probabilities (continuous lines) and 95% confidence envelopes (dotted lines). In **a** and **b**, the 5 largest observed annual maxima are dated and marked as filled circles.

5. CONCLUSIONS

This paper presents a brief study on the frequency analysis of floods at Apiúna, in the Itajaí-açu river, using the POT approach under nonstationarity. In order to study the influence of ENSO on the flood regime in that river, the Niño3.4 (DJF) climate index was used as a covariate. Following are the main conclusions obtained from the results.

- A significant influence of ENSO was found in both the Poisson parameter, λ, and the GP scale parameter, σ.

- Complex dependence structures were found between the covariate and the observed values of over-threshold occurrence counts, Y, and peak magnitudes, X_{OT}. As a result, the nonstationary model for annual maxima has a total of 8 parameters and comprehends a quadratic polynomial relationship on $\lambda(z)$, and a cubic polynomial relationship on $\sigma(z)$. Notwithstanding its large number of parameter, the model is parsimonious according to the LRT p-values and AIC scores.

- The methods applied in the analysis clearly demonstrate the advantages of nonstationary modeling of floods in a POT framework, namely, the ability to detect and model the influence of covariates on the occurrence process of floods, and their peak magnitudes separately, and using different dependence structures in order to obtain an annual maxima model that better describes the flood regime at the site.

The results of every step of the analysis were complemented with a comprehensive uncertainty analysis, through the construction of confidence envelopes for parameters and quantiles using the delta method.

6. REFERENCES

Abers, R. N., 2007. “Organizing for governance: building collaboration in Brazilian river basins”. *World Development*, 35(8), 1450-1463.

Akaike, H., 1974. “A new look at the statistical model identification”. *Automatic Control, IEEE Transactions on*, 19(6), 716-723.

Coles, S., 2001. *An introduction to statistical modeling of extreme values*. London: Springer.

Clarke, R. T., 2007. “Hydrological prediction in a non-stationary world”. *Hydrology & Earth System Sciences*, *11*(3).

Cunnane, C., 1979. “A note on the Poisson assumption in partial duration series models”. *Water Resources Research*, 15(2), 489-494.

Davison, A. C., 2003. *Statistical models*. Cambridge University Press.

Davison, A. C., and Smith, R. L., 1990. “Models for exceedances over high thresholds”. *Journal of the Royal Statistical Society. Series B (Methodological)*, 393-442.

Grimm, A. M., 2011. “Interannual climate variability in South America: impacts on seasonal precipitation, extreme events, and possible effects of climate change”. *Stochastic Environmental Research and Risk Assessment*, 25(4), 537-554.

Grimm, A. M., & Tedeschi, R. G., 2009. “ENSO and extreme rainfall events in South America”. *Journal of Climate*, 22(7).

Katz, R. W., 2010. “Statistics of extremes in climate change”. *Climatic Change*, 100(1), 71-76.

Katz, R. W., 2013. “Statistical methods for nonstationary extremes”. In *Extremes in a Changing Climate* (pp. 15-37). Springer Netherlands.

Martins, E. S. P., and Clarke, R. T., 1993. “Likelihood-based confidence intervals for estimating floods with given return periods”. *Journal of Hydrology*, *147*(1), 61-81.

Milly, P. C. D., Betancourt, J., Falkenmark, M., Hirsch, R. M., Kundzewicz, Z. W., Lettenmaier, D. P., and Stouffer, R. J., 2008. “Stationarity id Dead: Whither Water Management”. *Science*, *319*, 573-574.

NERC, 1975. *Flood Studies Report*, vol. I. Natural Environment Research Council.

Nery, J. T., Baldo, M. C., and Martins, M. D. L. O. F., 2008. “O comportamento da precipitação na Bacia do Itajaí”. *Acta Scientiarum. Technology*, *22*, 1429-1435.

Rayner, N. A., Parker, D. E., Horton, E. B., Folland, C. K., Alexander, L. V., Rowell, D. P., ... and Kaplan, A. (2003). “Global analyses of sea surface temperature, sea ice, and night marine air temperature since the late nineteenth century”. *Journal of Geophysical Research: Atmospheres (1984–2012)*, 108(D14).

Shane, R. M., and Lynn, W. R., 1964. “Mathematical model for flood risk evaluation”. *Journal of the Hydraulics Division*, 60(HY 6) 1-20.

Silva, A. T., Portela, M. M., and Naghettini, M., 2012. “Nonstationarities in the occurrence rates of flood events in Portuguese watersheds”. *Hydrology and Earth System Sciences*, *16*, 241-254.

Silva, A.T., Portela, M.M., and Naghettini, M., 2013. “On peaks-over threshold modeling of floods with non-zero inflated Poisson arrival under stationarity and nonstationarity”. *Stochastic Environmental research and Risk Assessment* (posted online ahead of print).

Tachini, M., 2010. *Avaliação de danos associados às inundações no município de Blumenau*. Ph.D. Thesis. Universidade Federal de Santa Catarina.

ACKNOWLEDGEMENTS

The authors wish to acknowledge the financial support to this research, provided by the agencies FCT, through a scholarship for A.T. Silva (grant SFRH/BD/86522/2012), and Fapemig.